Bulgarian Chemical Communications, Volume 58, Issue 1 (pp. 5-15) 2026 *DOI: 10.34049/bcc.58.1.5721*

Chemical characterization and performance analysis of post-modified microwave pyrolyzed karanja seed bio-oil

A. Mathiarasu[1*], S. Suresh Kumar[2], R. Senthil[3], R. Pandian[4]

[*1]*Department of Mechanical Engineering, Manakula Vinayagar Institute of Technology, Kalitheerthalkuppam 605107, Puducherry, India*

[2]*Department of Mechanical Engineering, PERI Institute of Technology, Mannivakkam, Chennai 600048, Tamil Nadu, India*

[3]*Department of Mechanical Engineering, C. Abdul Hakeem College of Engineering and Technology, Ranipet, Melvisharam 632509, Tamil Nadu, India*

[4]*Department of Mechanical Engineering, Dhanalakshmi Srinivasan University, Perambalur 621212, Tamil Nadu, India*

Received: September 11, 2025; Revised: October 21, 2025

Biomass has developed as a significant energy source capable of replacing regular fossil fuels such as coal and petroleum *via* different energy conversion methods. One such technique is pyrolysis, a process that thermally decomposes biomass in the absence of oxygen to produce valuable products. Microwave pyrolysis, which uses microwave energy to generate heat, is a method employed to convert non-edible biomass, like karanja seeds, into bio-fuel. To assess the efficacy of these bio-oil fuels, a Kirloskar four-stroke, single-cylinder, direct-injection diesel engine with a rated power output of 5.2 kW was used. The engine was tested with KB20, a blend of 20% karanja seed bio-oil and 80% diesel fuel, and EKB20 (post-modified bio-oil), a similar blend containing 20% karanja seed bio-oil and 80% diesel. The engine's performance was assessed based on cylinder pressure (PC), heat release rate (HRR) and brake thermal efficiency (BTE). The bio-oils produced from karanja seed microwave pyrolysis are dark brown and have a smoky odor. These bio-oils are significantly more viscous than diesel, with a calorific value of 27 MJ/kg—40 to 50% lower than that of diesel fuel. The assessments indicated that both KB20 and EKB20 blends resulted in increased PC and a faster HRR compared to diesel fuel. However, BTE decreased by 6.8% for KB20 and by 16.3% for EKB20 at maximum power output. Moreover, the use of these bio-oil blends led to higher concentrations of nitrogen oxides (NO_x) and increased smoke density relative to conventional diesel fuel.

Keywords: Diesel engine, Emulsification, Karanja bio-oil, Microwave pyrolysis, Thermal efficiency

INTRODUCTION

Biomass fuels are firmly produced from the biomass residues of wood products, agro-based crops, dried leaves, etc., which are considered to be some of the worldwide biggest renewable sources of energy that have a vast potential in order to replace some of the conventionally available energy sources like coal and petroleum. The application of bio-fuels in industrial [1, 2] and transportation sectors can reduce the release of gases like CO_2. Agronomic residues, engineering, aquatic and municipal solid wastes can be renewed into gaseous, and solid fuels by thermo-chemical or biotic processes [3, 4]. Non-edible seeds have an opportunity to be used in the manufacture of biofuels. Such waste can be turned into valuable chemicals and fuels by pyrolysis. Research works on the conversion of non-edible seeds into bio-fuels through conventional pyrolysis are reported. However, research works on microwave pyrolysis of non-edible seeds are not reported, yet though they are available for biomass like corn cob, palm waste [5-8] among transesterification, gasification, etc. The term "pyrolysis" refers to a process of heating and cooling in order to produce alternate fuels. Pyrolysis process here produces microwave irradiation which is employed as a heat source to convert the microwave energy to thermal energy. In microwave heating, uniform and rapid heating can be achieved as there is a volumetric heating of the material involved. However, it is effective only for selective materials [9-11].

Around 7.27 % of moisture content has been identified in the conventionally produced karanja seed bio-oil. This may be due to the lack of breaking of water molecules in the thermal decomposition which, when conventionally done, results in higher water content, i.e., moisture content of bio-oil. On the other hand, microwave pyrolysis results in creating bio-oil of lower humidity permitting its broad use. Even though there is appreciable moisture content in the feedstock for microwave pyrolysis which in turn reduces the necessity for removal of

* To whom all correspondence should be sent: Email: *mathiarasuanbu@gmail.com*

the moisture content in any biomass feedstock by means of microwave irradiation, the polarization of the molecules enables the collision of the water molecules improving the heating rate of the microwave pyrolysis heating process. This benefits the production of moisture-free karanja bio-oil by microwave pyrolysis in reducing knocking and delayed combustion during running of the engine, thus increasing its application [12, 13]. Emulsification is a highly effective method of enhancing fuel quality, providing the necessary stability to prevent phase separation and allowing the blending of sources [14]. Several non-ionic emulsifying agents exhibit remarkable efficiency in facilitating the emulsion process between bio-oil and diesel [15]. Hence, in this research, we capitalized on the presence of karanja seeds in the forested areas in and around Puducherry to generate karanja seed bio-oil using microwave pyrolysis. Subsequently, we employed an emulsion process to combine the bio-oil with diesel, ensuring the blend's stability for prolonged storage and enhancing the fuel's quality by eliminating moisture content *via* titration method.

EXPERIMENTAL

Karanja tree is drought-resistant, tolerates saline soils, and grows widely in tropical Asia.The non-consumable seeds of the Karanja trees are known for their rich oxygen content which is gathered from the woodland areas of Puducherry, India. The seeds shown in Figure 1 are brown, contain inside pods, and have a bitter taste.

Figure 1. Karanja seeds with pods

After carefully selecting the seeds, they are extracted from their shells and finely ground. The resulting powder is then sifted using a 1 mm mesh. To facilitate the emulsification process, various chemicals including diethyl ether, dichloromethane, Span 60, and Tween 60 were procured. These substances were selected based on their proven ability to enhance emulsion stability and efficiency. Diethyl ether and dichloromethane act as effective organic solvents, promoting the dispersion of hydrophobic components while Span 60 and Tween 60—nonionic surfactants—aid in reducing interfacial tension between oil and water phases. Their amphiphilic nature and compatibility with a wide range of formulation systems make them ideal for stable emulsion formation. This work conducted a comprehensive analysis of the karanja seeds, encompassing their proximate and elemental composition. This characterization aimed to provide insights regarding the behavior of the seeds during microwave irradiation and their subsequent thermal decomposition. The manufacture of karanja bio-oil by heat pyrolysis, was performed in an experimental setup using an LG Make internal microwave oven that activates at 2.45 GHz frequency and 800 W (28 × 12 × 10 cm). The oven was customized in such a way that it has appropriate holes for the connection of a N_2 gas cylinder, two aligned condensers and a thermocouple (k-type) for thermal investigation. The produced moist bio-oil mixture (pyrolytic liquid) is acquired by two conical flasks [16, 17]. Quartz was preferred as the primary material for the reactor due to its transparency to microwave radiation. This characteristic allows microwave energy to effortlessly penetrate within the reactor walls (made of quartz) and directly reach the sample without any energy loss. Additionally, quartz exhibits an exceptional heat resistance, capable of withstanding high temperatures up to 1600°C [18, 19]. Figure 2 displays karanja seed bio-oil.

Figure 2. Bio-oil formed by microwave pyrolysis

The pyrolytic oil formed by microwave pyrolysis of karanja seed is likely to contain clusters of various organic compounds and water molecules. Usage of the produced water-containing karanja bio-oil as a fuel in an engine affects the injection conditions of the engine, ignition and appearances [20, 21]. Moisture content plays a critical role in determining

the quality and stability of pyrolytic bio-oil, often contributing to undesirable phase separation during storage and handling. This phase split is primarily due to the polar nature of water, which interferes with the homogeneity of the bio-oil mixture. To address this challenge and better characterize the components of the bio-oil, a solvent-based separation technique was employed. In this study, the biologically derived compounds present in the produced bio-oil were isolated using a liquid-liquid extraction method involving dichloromethane (CH_2Cl_2). The latter, a non-polar organic solvent, is particularly effective in this application due to its ability to dissolve a broad range of organic compounds while remaining highly immiscible with water [22]. This selective miscibility facilitates efficient separation of water-soluble and organic-soluble fractions, enabling more accurate downstream analysis and processing of the bio-oil. The detailed methodology for this separation process, including phase behavior and solvent interactions, has been previously described in an earlier study [23].

The analysis of the pyrolytic bio-oil produced by karanja seeds revealed a heterogeneous mixture that contained both organic and inorganic components. To achieve a homogeneous blend of pyrolytic bio-oil and diesel, an emulsification technique using Span 80 and Tween 60 was employed to stabilize the immiscible liquids. The study exhibited that the bio-oil-diesel mixture remained stable for around 40 days [24], which later evaluated the long-term stability of pyrolysis oil (bio-oil) formulations in diesel fuel containing polyethylene glycol dipolyhydroxystearate. The produced bio-oil – diesel emulsion was further examined in detail in a previous publication [23]. Three kinds of fuels were verified in a single-cylinder diesel engine in the current study. The components and fuel list are shown in Figure 3.

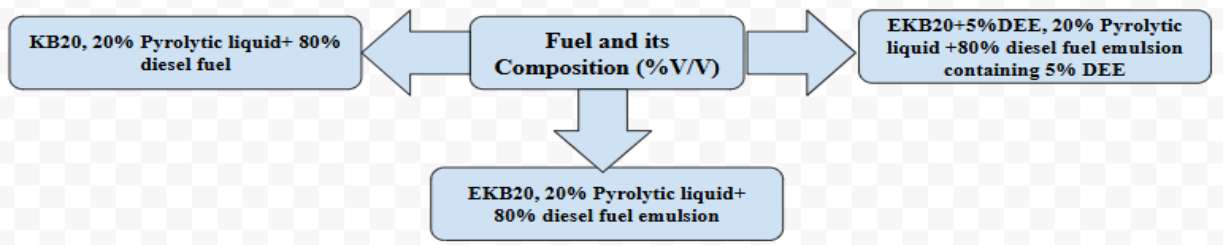

Figure 3. Fuel compositions used for research

The fuel characteristics of KB20 and EKB20 were assessed, encompassing measurements of viscosity using a rheometer, flash point utilizing a Cleaveland open cup device, high in calories value through a bomb calorimeter, and pH determined with a pH meter. FT-IR spectroscopy was used to study the functionally related makeup of KB20 and EKB20. The materials' infrared spectra were acquired in the 400-4000 cm^{-1} region with a 4 cm aspect ratio and 32 scans.

Experimental setup - engine

To investigate the efficiency, combustion process, and emission properties of diesel fuels, a single-cylinder, direct-injection diesel engine with a rated power output of 5.2 kW was used. During the analysis process, the engine was operated using the produced fuels, and various other parameters related to emissions were restrained for KB20, EKB20 and diesel as fuel. The engine specifications are shown in Figure 4. The experimental procedure began by utilizing diesel fuel as the initial test fuel for conducting experiments under different engine load conditions. Baseline data were gathered, enabling the calculation of engine characteristics. The measurement results presented on the control board were documented in conjunction with the load tests performed on different outputs. A number of alternative fuels were then used to power the engine, including KB20 and EKB20. Prior to switching to the unusual fuel, the engine was initially fed with diesel fuel and ran for 15 min.

Uncertainty analysis for the experiment

To determine the accuracy in an experiment involving any type of instrument, uncertainty analysis is done. Either fixed or random errors are measured in uncertainty analysis. Among both, random errors are hard to resolve in between the experiments and were statistically analyzed. In such cases researchers suggest an intention method to statistically analyze the indecision of each measurement. This error exploration permits to establish the accuracy of the new data.

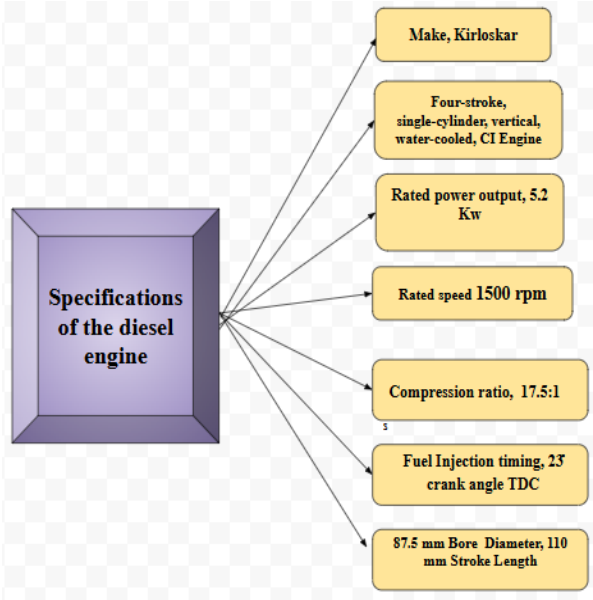

Figure 4. Specification of the engine

Uncertainty analysis was conducted to determine accuracy by measuring both fixed and random errors. Random errors were statistically analyzed using standard methods. For smoke opacity measurements at maximum brake power (5.2 kW), five trials were conducted with a mean value of 71.216 and standard deviation of 0.215128. This analysis establishes the reliability and accuracy of experimental data. Based on this, the accuracy of the values is hereby displayed in Figure 5 and Table 1.

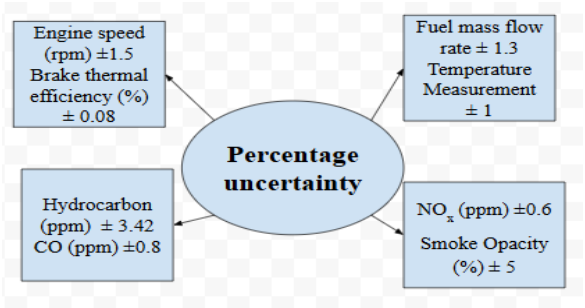

Figure 5. Evaluated uncertainty values at operating circumstances

Table 1. Uncertainty analysis for maximum brake power

Trials	Smoke opacity for max. brake power (5.2 kw)
X_1	71.12
X_2	71.1
X_3	71.6
X_4	71.12
X_5	71.14
Mean (X_i)	71.216
Standard deviation	0.215128

RESULTS AND DISCUSSION

Physicochemical properties

The obtained karanja seed bio-oil is dark brown, with smokey aroma, in nature comparing to the bio-oil produced by other types of pyrolysis processes resulting in prominent characteristics enabling to employ it in diesel engines by blending with diesel [25]. No data regarding the physical properties of the produced karanja seed bio-oil by other means of pyrolysis have been tabulated. The color differences result from the organic compounds present in the bio-oil, the blending process, and the post-modification treatment. The darker colors in bio-oil blends indicate the presence of complex organic molecules formed during pyrolysis. Based on the investigation of viscosity of karanja bio-oil and diesel, it is perceived that diesel has eight times lower energetic viscosity than karanja seed bio-oil. There is a connection between this phenomenon, fuel injection criteria and fuel properties. Viscosity affects fuel injection and atomization; flash point determines safety and ignition characteristics.

Table 2. Properties of bio-oil obtained by microwave pyrolysis of karanja seed

Attributes	Diesel	Karanja seed bio-oil	KB20	EKB20
Color	Tint green	Dark brown	Black	Caramel brown
Cetane number	49	30.11	41.36	45.14
Flash point (°C)	58	90	88	88
Calorific value (MJ/kg)	43.52	28.75	36.4	36.4
Dynamic viscosity (cP)	2.6	19	4.2	4.2

Compared with diesel, karanja seed bio-oil has lower fattening value and aniline point. The reduced aniline point of the produced fuel will reflect in ignition quality during running of the engine thereby with low cetane number. The lower cetane number of pure karanja bio-oil indicates poor ignition quality, which improves when blended with diesel. EKB20 shows better ignition quality than KB20 due

to the post-modification process that removes moisture and impurities. The comparative details are listed in Table 2 [11, 26, 27].

Fuel chemical composition

FTIR investigation was utilized to determine the functionalities of organic compounds found in KB20 and EKB20. Figure 6 displays the functional groups present in KB20, as determined through FTIR analysis, while Table 3 provides a comprehensive outline of the analysis. The FTIR spectral analysis of the KB20 sample reveals prominent absorption bands that indicate the presence of several key functional groups, suggesting a complex mixture of oxygenated and nitrogenated compounds in the bio-oil. Broad absorption peaks observed at 3340.1 cm^{-1}, 3191.6 cm^{-1}, and 3016.8 cm^{-1} correspond to the stretching vibrations of hydroxyl (–OH) and amine (–NH) groups. These are typically attributed to aliphatic primary and secondary amines, as well as alcohols, indicating the presence of polar compounds formed during pyrolysis. The occurrence of –NH stretching at 2923.8 cm^{-1} and 2864.4 cm^{-1} further supports the presence of amine salts or possibly hydrogen-bonded amines, which may arise from protein decomposition during thermal treatment of the karanja biomass [28, 29].

In addition, strong absorption bands at 1719.0 cm^{-1} and 1672.3 cm^{-1} are characteristic of carbonyl (C=O) stretching vibrations, typically associated with aldehydes, ketones, carboxylic acids, or esters—common pyrolysis products of lignocellulosic and lipidic materials [30]. The band near 1566 cm^{-1} corresponds to C=C stretching vibrations of alkenes or aromatic structures, suggesting the presence of unsaturated or aromatic hydrocarbons formed during thermal cracking. The coexistence of these functional groups highlights the chemically diverse nature of the pyrolytic bio-oil and suggests a combination of lignin-derived phenolics, fatty acid derivatives, and nitrogen-containing compounds originating from proteins or other nitrogenous components of karanja seed cake [31].

The C-H functional group and S=O functional group (at 1461.9 cm^{-1} and 1407.7 cm^{-1}, respectively) correspond to the bending and stretching vibrations of alkane and sulfonyl chloride, respectively. Additionally, the existence of CO–O–CO functional group (at 1047.7 cm^{-1}) suggests the formation of anhydride, which is indicated by its stretching vibration. The maximum IR absorbance is observed for the OH (phenol s) - stretching and C=C stretching, which correspond to the lignin elements. The spectra of the various samples also show the lignin unit's distinctive vibrations [32].

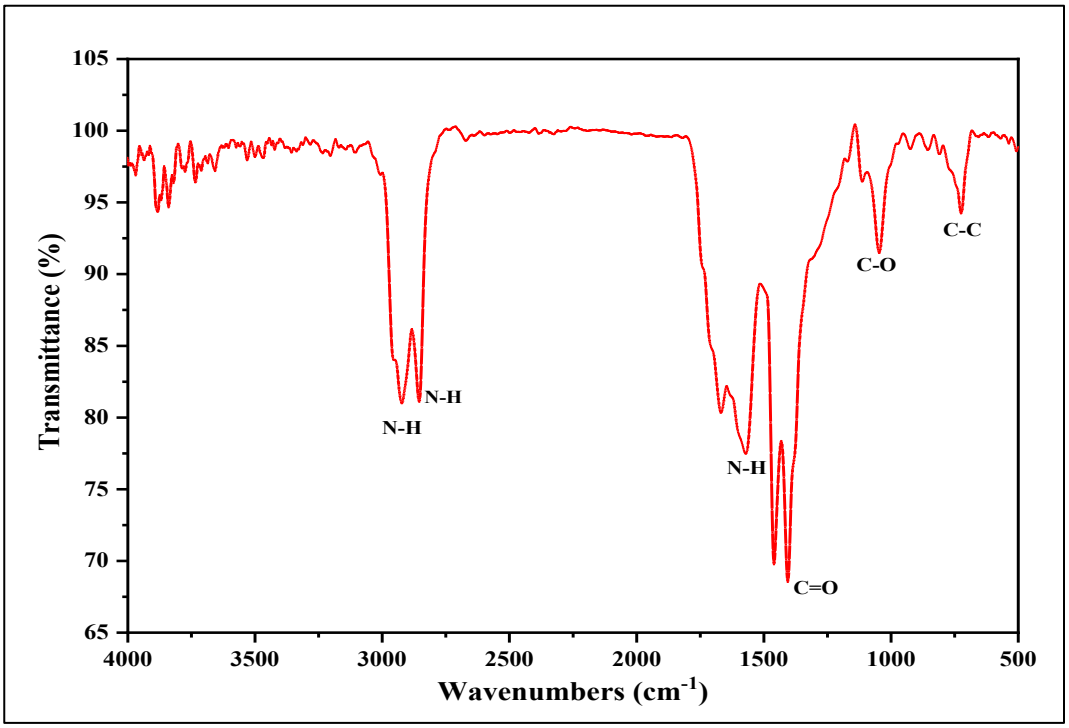

Figure 6. Functional groups of KB20 through FTIR.

Table 3. Functional groups in KB20

Wavenumber (cm^{-1})	Intensity / Appearance	Vibrational mode identified Stretching*/ Bending#	Functional group / Compound detected in karanja seed bio-oil
3340.1	Moderate	N–H*	Indicates presence of aliphatic primary amine
3181.6	Weak, Broad band	O–H*	Suggests alcohol functional group
2923.8	Strong, Broad absorption	N–H stretching	Corresponds to amine salt
2853.4	Strong, Broad absorption	N–H*	Associated with amine salt
1719.0	Intense Peak	C=O*	Represents carboxylic acid functionality
1672.3	Intense Peak	C=O*	Denotes conjugated acid group
1566.0	Moderate Peak	C=C*	Attributed to cyclic alkene structure
1461.9	Moderate Peak	C–H#	Typical of alkane compounds
1047.7	Broad, Strong band	CO–O–CO*	Corresponds to anhydride group

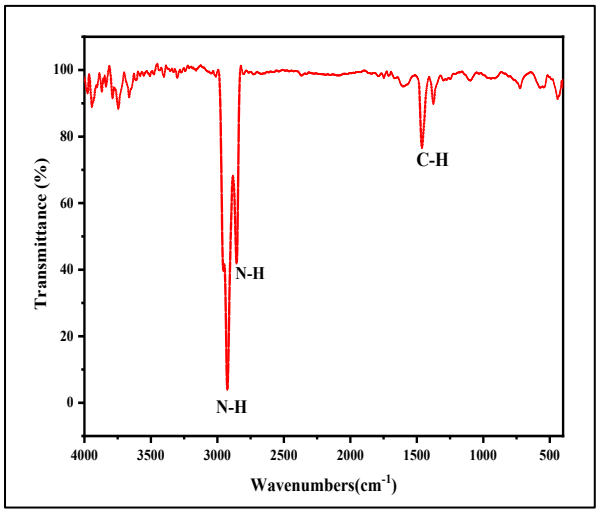

Figure 7. Functional groups of EKB20 through FTIR

Figure 7 displays the FTIR analysis results of EKB20, which is a bio-oil diesel emulsion, and Table 4 provides a detailed summary. The curves indicate the presence of N-H functional groups (at 2924.8 cm^{-1} and 2855.5 cm^{-1}) in EKB20, which can be accredited to the stretching atmospheres of amine salts compounds. Additionally, a functional group corresponding to C-H (at 1461.2 cm^{-1}) is perceived, related with alkane folding vibration [33, 34].

Table 4. Functional groups in EKB20

Wavenumber (cm^{-1})	Intensity / Appearance	Group Stretching*/ Bending# with compounds
2924.8	Strong & Broad	N-H* Amine salt
2855.5	Strong & Broad	N-H* Amine salt
1461.2	Medium	C-H# Alkane

Performance characteristics

- *Ignition delay (ID).* ID can be signified as the time delay, expressed in degrees of crank angle (°CA), that occurs among the initiation of injection and the onset of incineration within the engine. It represents the time with in the initial injection of fuel and the moment when combustion actually commences. This phenomenon is primarily influenced by the physicochemical properties of the fuel, its ignition quality (cetane number), as well as certain engine operating conditions. The IDs of KB20, EKB20 and diesel fuel are shown in Figure 8 for various brake control outputs. It is observed that in all fuels used for the testing, there is a drop-in ignition latency with a corresponding surge in braking power out. This kind of response is due to a decrease in the time causing the gasoline to disintegrate during mixing with air which happens when the degree of the gases rises at higher engine loads.

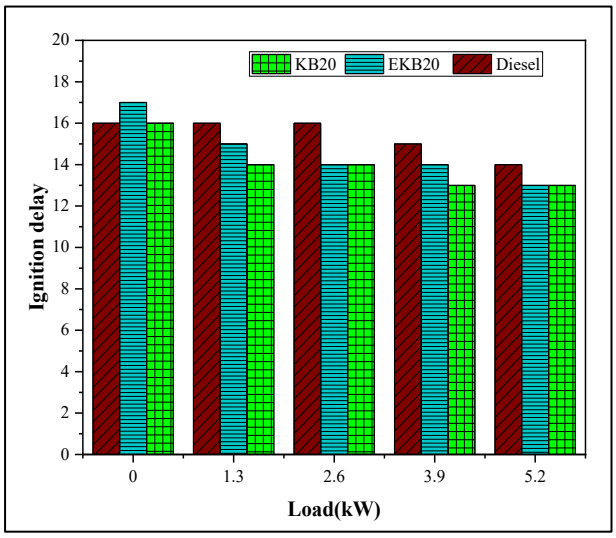

Figure 8. Variation of ID concerning brake power

This is due to the physicochemical properties, cetane number (ignition quality), and engine operating conditions. The incidence of moisture in fuel causes ignition delay, and the post-modification process in EKB20 helps reducing this effect. Ignition delay is observed for both EKB20 and KB20 on varying load. The prepared fuels EKB20 and KB20 exhibit a marginal moisture lower the moisture causing ignition delay in the fuel and the oil [35].

- *Cylinder gas pressure.* In Figure 9, a graphical representation of the pressure with respect to crank angle for different power outputs of the engine such as KB20, EKB20 and diesel fuel is plotted. For the prepared fuels (EKB20 and KB20), the peak pressure is higher in comparison to diesel fuel. The highest possible pressure for EKB20 is 75.86 bar, for KB20 is 72.40 bar and for diesel fuel it is 70.12 bar.

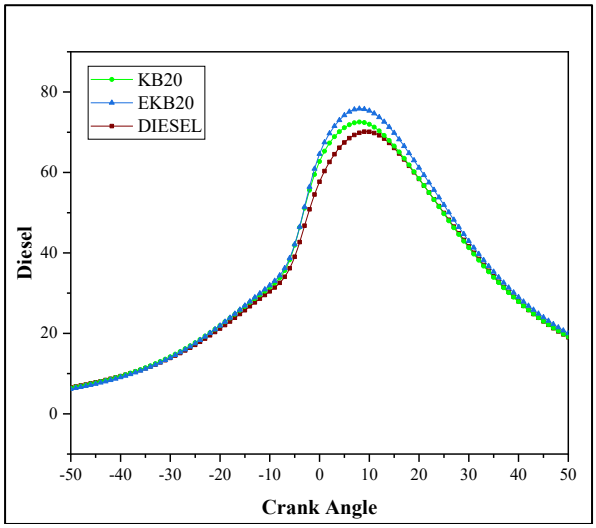

Figure 9. Variation of PC concerning crank angle

For EKB20 and KB20, in contrast with diesel, the peak gas pressure observed in the engine when using KB20 and EKB20 is found to be by 8% and 3% higher, correspondingly. It is essential to take into account that the peak pressure generated within the engine cylinder is chiefly determined by the quantity of fuel charred at the phase of the combustion process known as premixing. The prepared fuels EKB20 and KB20 have high peak pressure which is attained based on their lower energy content which needs larger quantities of fuel to be injected and burned during premixed combustion to produce the required power output. Therefore, for producing the required power output during the period of premixed combustion, a greater quantity of fuel gets injected and burned, which directly results in an increase in peak pressure when using respective fuels in the engine [36].

- *Net HRR.* Figure 10 illustrates the graphical representation of the net HRR at different power outputs for the prepared fuels EKB20, KB20 and also for diesel fuel in engine. The produced fuels EKB20 and KB20 exhibit the same heat release rate conditions as diesel fuel. Initially, owing to the vaporization of the fuel combination and the emission of heat, the heat release rate of the fuels causes a negative representation.

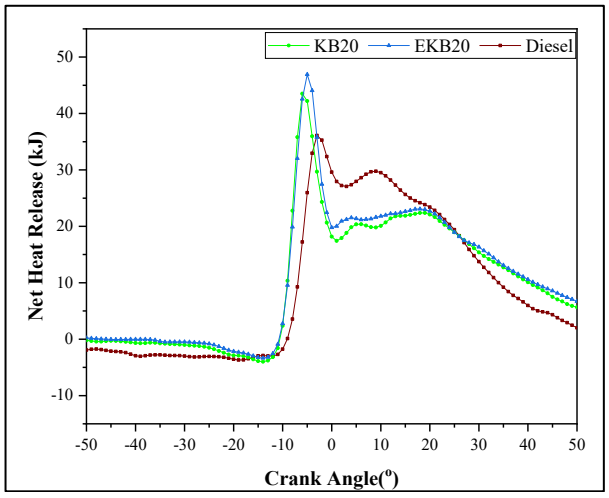

Figure 10. Variation of net HRR concerning crank angle

However, in the premixed incineration phase, heat release turns into positive, and also in the uncontrolled combustion point, heat release tends to result in uncontrollable situation during combustion. For all three fuels in the late combustion phase, it is experiential that there is a second peak in the HRR. On comparing diesel with KB20 and EKB20 fuels, the determined HRR occurred during the running of the engine in the rapid combustion phase. The maximum HRR for KB20 is 43.51 J/°CA, for EKB20 is 46.92 J/°CA and for diesel fuel it is 36.10 J/°CA. Due to the existence of oxygen-containing organic compounds a higher HRR was detected for the prepared fuels EKB20 and KB20. Further, when EKB20 fuel is used, micro-explosions may have developed, which automatically results in concentrated heat release rate. All three fuels show a second peak in the late combustion phase. Higher HRR in bio-oil blends is attributed to oxygen-containing organic compounds and potential micro-explosions in EKB20 [37].

- *Brake thermal efficiency.* Differences in brake thermal efficiency as a function of brake power for prepared KB20, EKB20 and diesel fuel for engine are represented in Figure 11. It is perceived that the engine produces lower BTE when EKB20 and KB20 are fueled in on comparing with fueling of diesel because of low energy density and high viscosity. For KB20 fuel, the brake thermal efficiency was 6.8% and for EKB20 fuel it was by 16.3% lower at the power output that is specified for the engine comparing to fuel. This reduction is due to the lower energy density and higher viscosity of bio-oil blends, which affect combustion efficiency and require more fuel to produce the same power output [38-40].

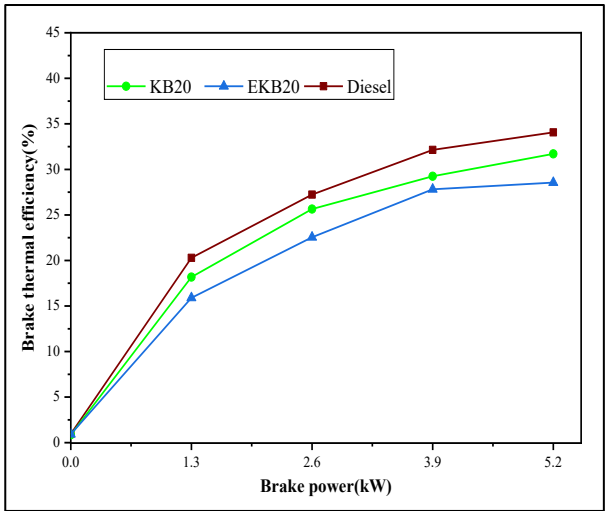

Figure 11. Variation in BTE concerning brake power output

- *Specific fuel consumption (SFC).* The mass or volume of fuel that is spent for a certain amount of time by an engine to produce a particular amount of engine braking power is referred to as the engine's particular use of fuel. It is a technical measurement that quantifies the fuel efficiency of an engine. The differences in the SFC for rated brake power outputs for prepared fuels KB20, EKB20 and for diesel fuel are represented in Figure 12. The SFC is noted to be by 20% greater in value for KB20 and by 36% greater when EKB20 fuel is used in the engine. The high viscosity nature of the prepared fuel KB20 and EKB20 increased the amount of gasoline that the engine required in order to develop the necessary power output. The high-viscosity nature of bio-oil blends increases the amount of fuel required to develop the necessary power output, leading to higher fuel consumption rates [20].

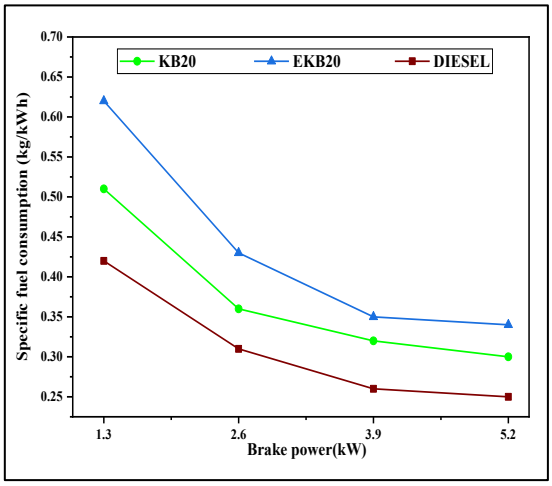

Figure 12. Variation in SFC concerning brake power output

Smoke opacity

Smoke zones constituted in the engine are based on higher fuel viscosity, poor fuel atomization, inadequate ignition that arises in fuel-rich zones, lower fuel volatility, and inappropriate fuel-air mixture. Figure 13 represents the differences in smoke opacity of EKB20, KB20 and diesel fuel. Due to the formation of fuel-rich zones because of enormous addition of fuel with increase in brake power the smoke opacity gets increased. It is perceived that the smoke density with EKB20 and KB20 is by 15% and 13% higher in value when comparing with diesel fuel at all rated power outputs. These differences are due to the development of organic compounds with higher molecular mass and the smoke formation is caused by higher fuel viscosity, poor fuel atomization, inadequate ignition in fuel-rich zones, lower fuel volatility, and inappropriate fuel-air mixture. The development of organic compounds with higher molecular weight also contributes [41, 42].

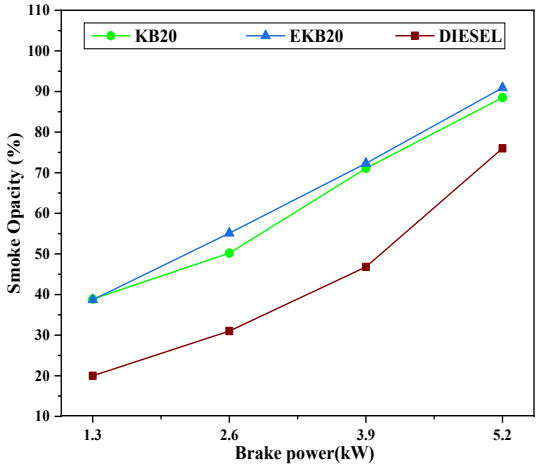

Figure 13. Variation of smoke opacity concerning brake power output

NO_X emission

NO_x emissions are technically described as a blend of nitric oxide (NO) and nitrogen dioxide (NO_2), with NO being the primary nitrogen oxide formed during the ignition of fuel in a diesel engine. Nitrogen, when exposed to temperatures higher than 1500 °C, will react with oxygen (O_2) to produce nitrogen oxides (NO_x). There is a correlation between decreased radiating heat transfer, raised flame temperature, quick HRR, and sufficient supply of oxygen in the combustion zones. All of these factors lead to enhanced NO_x generation [43, 44]. The variation in NO_x formation in engines operating with different brake power outputs is compared for KB20, EKB20, and diesel fuel in Figure 14. In this emission analysis it is noted that by increasing the brake power the output reacts in an increase of temperature during the combustion process built on the admission of excess fuel into the incineration chamber resulting in an increase of NO_x during the combustion process. It is found that there are higher NO_x concentrations for both KB20 and EKB20 associated to diesel at all loads. At the peak brake power output, the NO_x emission was observed to be by 26% higher for both KB20 and EKB20 compared to diesel. This is related to the higher HRR of KB20 and EKB20 when equated to diesel fuel [2]. This increase correlates with the higher heat release rates of bio-oil blends, elevated combustion temperatures, reduced heat transfer, and adequate oxygen supply in combustion zones, all contributing to enhanced NO_x formation above 1500°C [37-39].

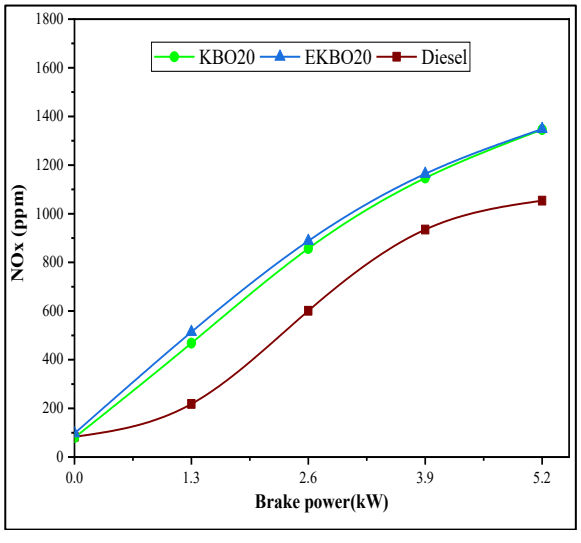

Figure 14. Variation of NO_x concerning brake power output

CO emission

Because of the inadequate burning of carbon in the fuel, CO emissions are produced. In general, diesel engines function with an air-fuel ratio that is considered low under various load conditions, leading to significantly lower CO emissions compared to spark-ignition (SI) engines. Figure 15 illustrates CO emissions at different engine brake power outputs. It is evident that the CO emission is highest at all rated power outputs for the verified fuels. This can be attributed to the injection of a higher amount of fuel during the rated power output, resultant in a higher fuel-to-air ratio. This, in turn, leads to incomplete or improper combustion, causing an increase in CO releases. EKB20 is by 20% higher and KB20 is by 8% lower when compared to diesel fuel.

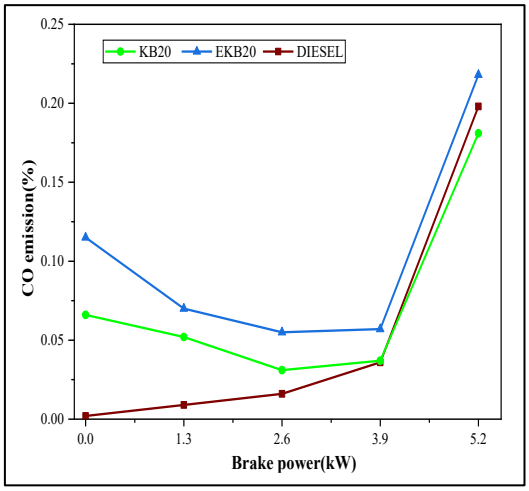

Figure 15. Variation of CO concerning brake power output

This might be due to the more viscous nature of the bio-oil blends which deliberately results in the development of larger droplets of the fuel used and is also due to incomplete combustion [45]. Also, CO emissions result from inadequate carbon combustion and increase with power output due to higher fuel injection rates creating higher fuel-to-air ratios. The more viscous nature of bio-oil blends leads to larger fuel droplets and incomplete combustion [43].

Hydrocarbon emission

Unburned hydrocarbons are mostly formed when fuel is trapped in different engine mechanisms in an internal combustion engine running diesel. Vital aspects such as indecorous evaporation of fuel and fuel-rich zone correspondingly end in higher development of unburned hydrocarbons. Figure 16 shows the alterations in the emission of hydrocarbons for various power outputs. With gradual increasing the power outputs it is observed that here is a subsequent increase in hydrocarbon emission for all the fuels prepared. Because of the charge consistency and advanced oxygen availability at the lower loads there is lower

emission, whereas on increasing load conditions the emissions are high because of the high quantity of fuel injected during the combustion process. It is also observed that there is high hydrocarbon emission on comparing to the diesel fuel for both EKB20 and KB20 (Figure 16.

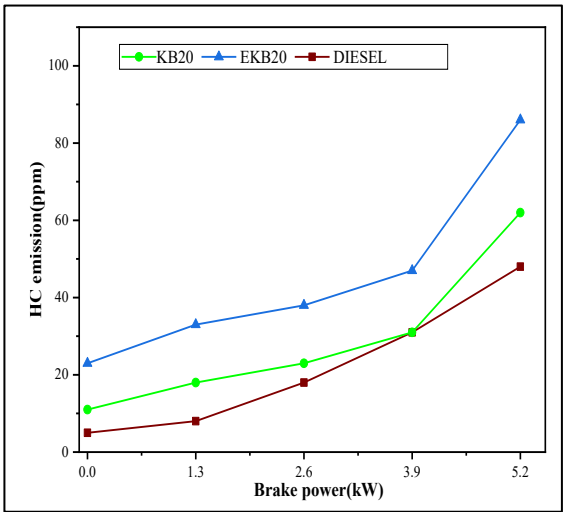

Figure 16. Variation of HC concerning brake power output.

This phenomenon can be due to the increased latent heat of humidity present in the fuel, which vaporizes during combustion. This leads to flame quenching, particularly at the combustion chamber walls of the engine, resulting in incomplete combustion. As a result, at the rated power outputs, the hydrocarbon emissions for EKB20 are observed to be 79% compared to diesel fuel, while for KB20, the increase is by 29% higher related to diesel fuel. This increase is attributed to the presence of moisture in the fuel, which increases the latent heat during vaporization, leading to flame quenching at the combustion chamber walls and resulting in incomplete combustion [36].

CONCLUSIONS

This investigation successfully demonstrated the viability of converting non-edible karanja seeds into bio-oil through microwave pyrolysis, yielding a dark brown product with characteristic smoky odor. Comprehensive physicochemical characterization established that while bio-oil exhibited viscosity approximately eight times higher than that of conventional diesel, its calorific value of 28 MJ/kg—though by 40-50% lower than diesel—remains within acceptable ranges for biofuel applications. The enhanced viscosity can be attributed to the presence of long-chain fatty acids and oxygenated compounds inherent to pyrolytic bio-oils, which also contribute to improved lubricity properties beneficial for engine components. Engine performance trials with EKB20 and KB20 fuel blends revealed favorable combustion characteristics, including elevated cylinder pressure and accelerated heat release rates, indicating more efficient fuel-air mixing and combustion propagation. These findings suggest improved atomization and combustion kinetics despite the physicochemical differences from petroleum diesel. Although brake thermal efficiency decreased by 6.8% for KB20 and by 16.3% for EKB20 relative to baseline diesel at rated power output, these reductions are considerably modest given the renewable nature of the fuel source and can be offset through minor engine optimization strategies such as injection timing adjustment or compression ratio modification. The observed increases in NO_x emissions and smoke density during combustion of both blends align with typical biofuel combustion patterns, where higher oxygen content promotes elevated combustion temperatures conducive to thermal NO_x formation, while incomplete combustion of heavier molecular fractions contributes to particulate matter generation. These emissions remain manageable through exhaust gas recirculation systems or selective catalytic reduction technologies already employed in modern diesel engines. Significantly, this study validates the technical feasibility of utilizing karanja-based biofuels as sustainable alternatives to fossil diesel, particularly advantageous considering karanja's non-edibility. Therefore, karanja seed-derived bio-oil blends represent promising, environmentally responsible fuel alternatives warranting further development and commercialization for sustainable energy transition in compression ignition engines.

Acknowledgement: *Not applicable.*
Author contributions: *The authors have accepted responsibility for the entire content of this manuscript and approved its submission.*
Conflict of interest: *On behalf of all authors, the corresponding author states that there is no conflict of interest.*
Research funding: *Not applicable.*
Data availability: *Not applicable.*

REFERENCES

1. J. H. Chang, S. Selvaraj, S. Manikandan, S. Nagarani, A. Senthilkumar, M. S. Samuel, E. Selvarajan, A. J. John, M. Kumar, *Biomass Conv. Bioref*., **202**, 108167 (2025).
2. A. A. Azni, W. A. W. A. K. Ghani, A. J. Idris, M. F. Z. a'afar, M. A. M. Salleh, N. S. Ishak, *Renew. Energy*, **142,** 123 (2019).
3. C. B. John, S. Baskar, *Fuel,* **405,** 136627 (2026).
4. J. P. Pandian, M. Pugazhvadivu, B. Prabu, K. Velmurugan, V. S. K. Venkatachalapathy, *Jordan J. Mech. Ind. Eng.,***15,** 273 (2021).
5. A. V. Bridgwater, G. V. C. Peacocke, *Renew. Sustainable Energy Rev.*, **4,** 1 (2000).
6. A. M. Al-Qahtani, *Energies, 1***6,** 6876 (2023).
7. A. Alcala, A. V. Bridgwater, *Fuel*, **109**, 417 (2013).
8. A. V. Bridgwater, *Catal. Today*, **29**, 285 (1996).
9. F. Yu, S. Deng, P. Chen, Y. Liu, Y. Wan, A. Olson, D. Kittelson, R. Ruan, *Appl Biochem Biotechnol.,* **137,** 957 (2007).
10. C. Wu, V. L. Budarin, M. J. Gronnow, M. De Bruyn, J. A. Onwudili, J. H. Clark, P. T. Williams, *J. Anal. Appl. Pyrolysis,* **107**, 276 (2014).
11. A. Mathiarasu, M. Pugazhvadivu, *Biomass Conv. Bioref*., **13**, 2895 (2023).
12. F. Mushtaq, R. Mat, F. N. Ani, *Renew. Sustain. Energy Rev*., **39**, 555 (2014).
13. F. Motasemi, A. A. Salema, M. T. Afzal, *Trans. ASABE.*, **58,** 869 (2015).
14. A. Farooq, H. Shafaghat, J. Jae, S. C. Jung, Y. K. Park, *J. Environ. Manage.,* **231**, 694 (2019).
15. Z. Guo, S. Wang, X. Wang, *Energy.,* **66,** 250 (2014).
16. A. Mathiarasu, M. Pugazhvadivu, *AIP Conf. Proc*., 2225, 040002 (2020).
17. A. Mathiarasu, M. Pugazhvadivu, *IOP Conf. Ser.: Earth Environ. Sci.,* **312**, 012022 (2019).
18. E. Antunes, M. V. Jacob, G. Brodie, P. A. Schneider, *J. Anal. Appl. Pyrolysis,* **129**, 93 (2018).
19. F. Motasemi, M. T. Afzal, A. A. Salema, J. Mouris, R. M. Hutcheon, *Fuel,* **124**, 151 (2014).
20. S. I. Yang, M. S. Wu, C. Y. Wu, K. H. Chen, T. M. Wu, Y. L. Hsu, Y. Y. Ku, *Adv. Mater. Res.*, **591**, 325 (2012).
21. A. K. Hossain, P. A. Davies, *Renew. Sustain. Energy Rev.,* **21**, 165, (2013).
22. T. Aysu, *Bioresour. Technol.,* **191,** 253 (2015).
23. M. Anbu, R. Balakichenin, P. Muthaiyan, S. Sundaramoorthy, K. T. T. Amesho, V. Subramani, *Environ. Sci. Pollut. Res.,* **30**, 125006 (2023).
24. J. A. Martin, C. A. Mullen, A. A Boateng, *Energy Fuels*, **28**, 5918 (2014).
25. A. S. Ahmed, *Int. J. Renew. Energy Res*., **13**, 14 (2023).
26. N. K. Nayan, S. Kumar, R. K. Singh, *Bioresour. Technol.,* **124**, 186 (2012).
27. K. P. Shadangi, K. Mohanty, *Renew. Energy,* **63**, 337 (2014).
28. A. A. Salema, F. N. Ani, *APCBEE Procedia*, **3,** 188 (2012).
29. F. Stankovikj, A. G. McDonald, G. L. Helms, G. P. Manuel, *Energy Fuels*, **30**, 6505 (2016).
30. S. Black, J. R. Ferrell, *Energy Fuels*, **30**, 1071 (2016).
31. S. Hosseinnezhad, H. F. Ellie, K. S. Brajendra, B. Mufeed, K. Bidhya, *RSC Adv.*, **5**, 75519 (2015).
32. L. Rosi, M. Bartoli, M. Frediani, *Waste Manag.,* **73,** 511 (2018).
33. B. Biswas, N. Pandey, Y. Bisht, R. Singh, J. Kumar, T. Bhaskar, *Bioresour. Technol.,* **237**, 57 (2017).
34. M. Bartoli, L. Rosi, A. Giovannelli, P. Frediani, M. Frediani, *J. Anal. Appl. Pyrolysis*, **119**, 224 (2016).
35. M. Mohamed, C. K. Tan, A. Fouda, M. S. Gad, O. Abu-Elyazeed, A. F. Hashem, *Energies*, **13**, 5708 (2020).
36. S. Sivalakshmi, T. Balusamy, *Fuel,* **106,** 106 (2013).
37. M. Mani, G. Nagarajan, S. Sampath, *Fuel*, **89**, 1826 (2010).
38. R. Prakash, R. K. Singh, S. Murugan, *J. Energy Inst.,* **88,** 64 (2015).
39. A. Zahir Hussain, A. Santhoshkumar, A. Ramanathan, *J. Therm. Anal. Calorim.,* **141**, 2277 (2020).
40. V. Volli, R. K. Singh, S. Murugan, *Waste Biomass Valor.,* **5,** 661 (2014).
41. R. Sinha, S. Kumar, R. K. Singh, *Biomass Conv. Bioref.,* **3**, 327 (2013).
42. R. Prakash, R. K. Singh, S. Murugan, *Energy*, **55,** 610 (2013).
43. I. Kalargaris, G. Tian, S. Gu, *Fuel.,* **211**, 797 (2018).
44. I. Kalargaris, G. Tian, S. Gu, *Fuel Process. Technol.*, **161,** 125 (2017).
45. N. Vedaraman, S. Puhan, G. Nagarajan, K. C. Velappan, *Int. J. Green Energy,* **8,** 383 (2011).